Sources of continuous tremor associated with jökulhlaups and eruptions of Grímsvötn volcano, Iceland

Páll Einarsson[1], Finnur Pálsson[1], Magnús Pálsson[1], Eyjólfur Magnússon[1],
Bryndís Brandsdóttir[1] and Tom Winder[1,2]

[1]*Institute of Earth Sciences, Science Institute, University of Iceland, Reykjavík, Iceland*

[2]*Bullard Laboratories, University of Cambridge, Cambridge, UK*

Corresponding author palli@hi.is; https://doi.org/10.33799/jokull2023.73.055

Abstract — *The Grímsvötn volcano, one of the most active volcanoes in Iceland, is covered to a large extent by the Vatnajökull glacier. High geothermal activity within its caldera maintains an ice-covered caldera lake with variable water level. Large floods from the lake (jökulhlaups) are initiated when the water breaks through an ice dam and flows out of the caldera. In several cases the falling lake level is known to have triggered eruptions of the volcano, e.g, in 1922, 1934, and 2004. The eruptions of 1983, 1998, and 2011, however, were not triggered by jökulhlaups, and most jökulhlaups have not triggered eruptions, including those of 2008 and 2010. All these processes, i.e. volcanic activity, water floods, and geothermal activity, are accompanied by seismic tremor that is detectable by the surrounding network of seismic stations. By comparing tremorplots of the jökulhlaups of 2008 and 2010, and the eruptions of 2004 and 2011, we can identify three types of tremor:* Water flood tremor. *Jökulhlaups from the caldera are always accompanied by high-frequency tremor (2–9 Hz), recorded on the seismic stations near the caldera. It starts when the lake level begins to drop and increases gradually with increasing water discharge from the lake. This tremor is usually detected a few days before the subglacial flood reaches the glacier edge.* Geothermal tremor. *The second type of tremor appears to be switched on when the drop in water level reaches 10–30 m. It remains after all water has been drained from the lake. The tremor is characterized by relatively high frequency (2–6 Hz) and sudden changes in amplitude. The distance range of this tremor is short, it is seldom recorded beyond the edge of the glacier. We suggest that it is generated by flash-boiling of the geothermal system within the caldera, triggered by the pressure drop of the lake level.* Eruption tremor. *Eruptions of Grímsvötn are accompanied by tremor that begins simultaneously with the eruption and is distinctly different from the other two types of tremor. It contains lower frequencies (0.5–4 Hz) and has a wider distance range. It is recorded beyond the edge of the glacier, possibly because of its frequency content, but other effects such as crustal structure and depth of the tremor sources may also play a part.*

INTRODUCTION

The Grímsvötn volcano is located in the central area of the Iceland hotspot and is one of the most active volcanoes in Iceland (e.g., Björnsson and Einarsson, 1990; Gudmundsson and Björnsson, 1991). The latest confirmed eruptions were in 1922, 1934, 1983, 1998, 2004 and 2011. The volcano is to a large extent covered by the Vatnajökull glacier. Powerful geothermal

activity in the caldera of the volcano melts the ice and the meltwater feeds an active caldera lake. Glacier ice dams the lake but the dam eventually fails, resulting in a jökulhlaup, a major flood that reaches the coastal area in several hours to days (Björnsson, 1988; 2010). The caldera lake level drops by several tens of meters during these floods. The ensuing pressure drop in the caldera has been shown to trigger erup-

tions of the volcano, such as in 1922, 1934 and 2004 (Þórarinsson, 1974; Sigmundsson and Gudmundsson, 2004; Vogfjörð *et al.* 2005). Both the jökulhlaups and the eruptions have been accompanied by characteristic seismic activity, both earthquakes and continuous tremor (e.g. Einarsson and Brandsdóttir, 1984; Brandsdóttir and Einarsson, 1992; Vogfjörð *et al.* 2005; Einarsson, 2018; 2019). The eruptions have also followed a characteristic inflation-deflation cycle of a shallow-level crustal magma chamber (Sturkell *et al.*, 2003, 2006; Sigmundsson *et al.* 2018; Hreinsdóttir *et al.* 2014). This intriguing interaction of volcanological, geothermal, hydrological and seismic phenomena offers unique opportunities for research. In this paper we investigate continuous tremor signals in conjunction with recent eruptions and jökulhlaup events. We identify three kinds of tremor signals and tentatively trace their origin to water flow, flash boiling of the geothermal system, and volcanic eruptions. Detecting seismic tremor and identifying its origin is of paramount importance for volcano monitoring in Iceland. Several of the most active and dangerous volcanoes are covered by glaciers, such as Grímsvötn, Bárðarbunga, Skaftá Cauldrons, and Katla (Figure 1), and bursts of tremor are frequently detected from them (Einarsson and Brandsdóttir, 1984; Björnsson and Einarsson, 1990; Einarsson *et al.* 1997; Sgattoni *et al.* 2017; Eibl *et al.* 2020; Vanderhoof, 2023). In some of the cases it has been suggested that tremor bursts observed to distances of several tens of kilometers are indications of short-lived volcanic eruptions at the base of the glacier (Björnsson and Einarsson, 1990; Sgattoni *et al.* 2019), but direct evidence to verify or disprove the suggestion is missing.

METHODS

Seismic networks

The seismicity of Grímsvötn has been monitored since 1976–1977, when the country-wide analog seismograph network was extended to Eastern Iceland and events of magnitude as small as 2 could be located with reasonable accuracy in Central Iceland (Björnsson and Einarsson, 1990). A telemetered station was installed on the Grímsvötn caldera rim in 1982 (Figure 2) and operated intermittently in the following years (Einarsson and Brandsdóttir, 1984). These stations added considerably to the general knowledge of tremor and background activity of the volcano. The analog data do not, however, allow studies of spectral characteristics. Analog seismograms from the Grímsvötn station (ICGF) for the period 1986–2008 are available at the website seismis.hi.is (Einarsson and Jakobsson, 2020).

The analog seismic network of Iceland was replaced by a digital network, beginning in 1990 (Stefánsson *et al.*, 1993). The last analog station was taken out of operation in 2010. A digital, three-component seismic station was installed on the caldera rim of Grímsvötn in 1999, as a part of the country-wide digital seismic network (e.g., Böðvarsson *et al.* 1999). This station opened the possibilities to monitor continuous tremor in a quantitative way. In particular, tremorgraphs for most stations are routinely maintained on the webpage of the Icelandic Meteorological Office for the previous 10 days, http://hraun.vedur.is/ja/oroi/index.html. These graphs give the running one minute average microseismic background (RMS) of ground velocity measured on the vertical instrument in three different spectral bands, high-frequency band 2–4 Hz, intermediate band 1–2 Hz, and low-frequency band 0.5–1 Hz. The numbers on the Y-axis on the web images are the logarithm of the average velocity in m/s, scaled to a whole number between −32000 and 32000 (16 bit number) (Einar Kjartansson, pers. comm.).

We base our analysis of the Grímsvötn tremor mostly on tremorgraphs from the Grímsvötn station, GRF, for four key events, the jökulhlaups of 2008 and 2010, and the eruptions of 2004 and 2011. The advantage of using these data is twofold. The data are easily accessible and the results are immediately applicable to the routine monitoring of the volcano. Many people in the public community are already familiar with this presentation of the data. Community participation is an important element in the monitoring of the volcanic activity in Iceland. The tremorgraphs have been used for almost three decades to identify the start of jökulhlaups and issue early warning.
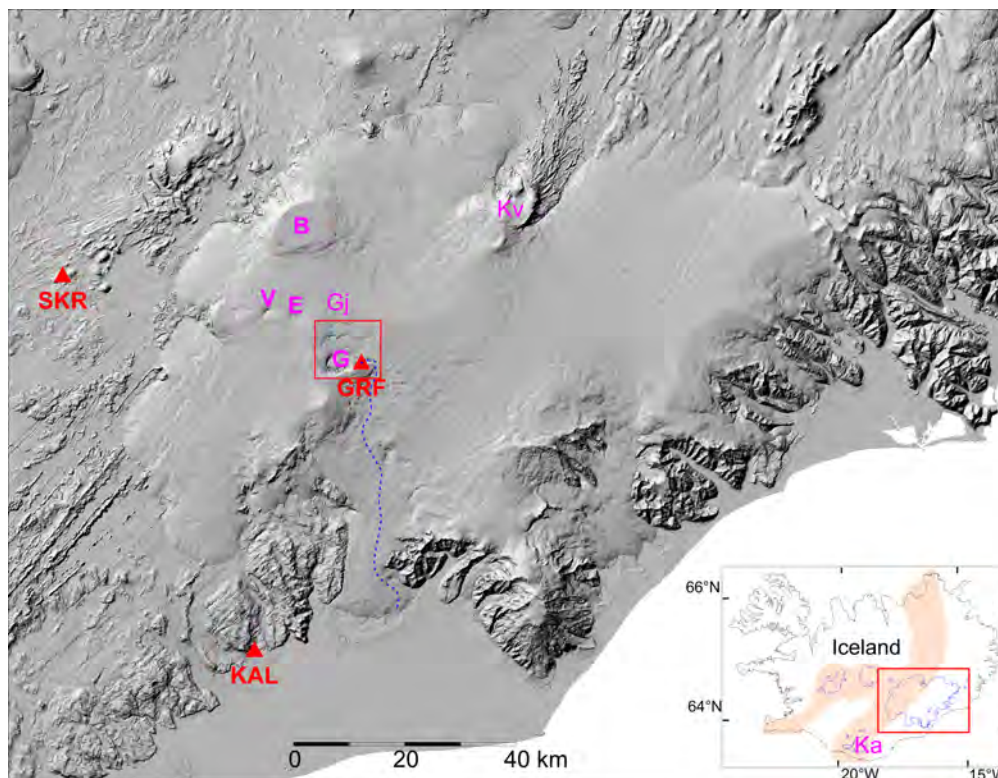
Figure 1. Map of the Vatnajökull area of Central and SE-Iceland, showing the location of the Grímsvötn volcano (G) and other volcanic features, Bárðarbunga (B), W- and E-Skaftá Cauldrons (V and E), Gjálp eruption site (Gj), Kverkfjöll volcano (Kv), and Mýrdalsjökull glacier with the subglacial Katla volcano (Ka). Seismic stations are shown with red triangles, Grímsfjall (GRF), Skrokkalda (SKR), and Kálfafell (KAL). – *Kort af Vatnajökli og nágrenni sem sýnir staðsetningu Gríms-vatna (G), Bárðarbungu (B), Vestri og Eystri Skaftárkatla (V og E), Gjálpar (Gj), Kverkfjalla (Kv), einnig Mýrdalsjökuls og Kötlu (Ka).*

The three spectral bands are sensitive to different environmental phenomena. The high-frequency band shows well local earthquakes, icequakes, water tremor from rivers, surf on the beach, wind noise, traffic noise, etc. The low-frequency band is sensitive to microseisms of the ocean (sometimes called "the 7-seconds microseisms") caused by ocean waves due to passing low-pressure systems in the atmosphere. The high-frequency tail of this spectral peak often contains sufficient wave energy to severely disturb this band of the tremorgraphs. Large teleseismic events and low-frequency volcanic earthquakes are also seen on this spectral band.

Lake level

Following experimental installations in the early 1990's, instruments to monitor the vertical height of the ice shelf floating on the Grímsvötn caldera lake were installed on the middle of the ice shelf in late October 1996 (Figures 2 and 3). Since then an almost continuous record of water level in the Grímsvötn caldera exists. The instruments record atmospheric pressure and air temperature. Similar instruments record the pressure and temperature at Grímsfjall, the research hut of the Glaciological Society on the southern caldera rim. The height difference between the hut and the top of the ice shelf is calculated from

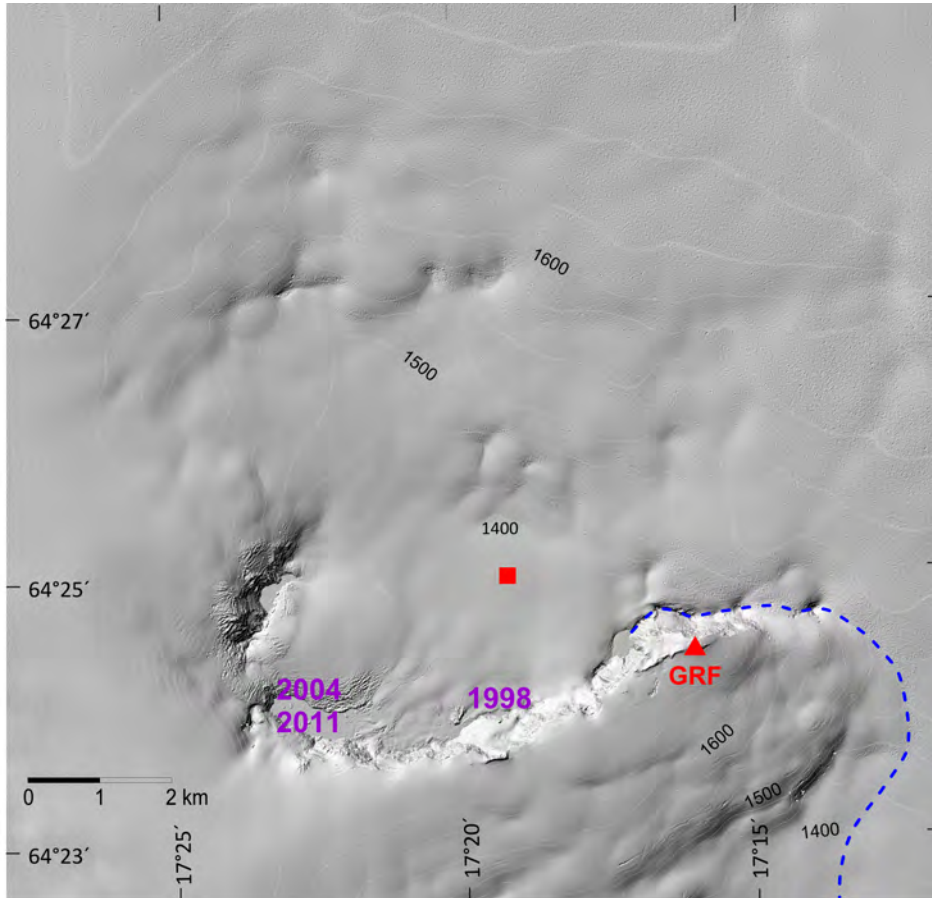$$dz = (T_0/\gamma) \times [1 - (P/P_0)(R\gamma/g)]$$

Figure 2. A shaded relief map of Grímsvötn, made from a digital elevation model (DEM), dated 2017 08 24 (Porter *et al.*, 2018). The eruption sites of 1998, 2004, and 2011 are shown and the outflow channel for the jökulhlaups is indicated with a dashed line. The red triangle gives the location of the seismograph, the square the location of the measuring station for the height of the ice shelf. – *Skuggamynd hæðarlíkans af Grímsvötnum, úr Arctic DEM safninu. Gosstöðvar frá 1998, 2004 og 2011 eru merktar. Brotin lína sýnir rennslisleið jökulhlaupa út úr öskjunni. Þríhyrningur sýnir staðsetningu skjálftamælisins á Grímsfjalli. Rauður ferningur sýnir staðsetningu hæðarmælis á íshellunni.*

where T_0 and P_0 are temperature [K] and atmospheric pressure [Pa] at Grímsfjall, γ is the temperature gradient [K/m], P atmospheric pressure [Pa] on the ice shelf, g is the acceleration of gravity [m/s^2], and R is the specific gas constant for dry air [J kg^{-1}K^{-1}].

The accuracy of these measurements is about 5 m in elevation for individual measurements. Each segment of the time series is constrained at both ends by elevation measurements by GPS that have uncertainties of the order of 1 m or less. It is assumed that the

water level is 30 m below the surface of the ice shelf. An indirect measurement of the water level is thus obtained.

In 1998 a water pressure gauge was deployed at the lake bed through a borehole drilled through the $\sim$260 m thick ice shelf at the monitoring station. This allowed monitoring of the water-level with decimeter accuracy. The device was destroyed during the Grímsvötn eruption in December 1998. A new instrument was installed in June 1999 at a location 800 m

to the ENE of the previous site. This gauge was in operation until late August 2000, when the cable to the surface station broke. Since June 2000 the elevation of the ice-shelf has been monitored more or less continuously with GNSS instruments of variable accuracy from a few meters to a few cm.

The volume of the water body of the lake as a function of the water level is estimated from maps of the topography of the lake bottom and the bottom of the ice shelf. The volume of each jökulhlaup is estimated as the difference between the volume of the lake at the beginning and that at the end of the jökulhlaup. The jökulhlaup following the Gjálp eruption of 1996 serves as an example. The water level before the outflow began was at 1513 m and at the end of the flood it was at 1335 m. The calculated volume of the flood is 3.6 km^3.

In 1999, the monitoring station was moved to a new location directly above the deepest part of the subglacial lake. Consequently, if any water accumulated in the lake, the ice below the station was lifted from the bedrock below, and when the lake drained the ice shelf at the station subsided until the lake drainage stopped. Since the eruptions of 1996 and 1998, the elevation of the station when the ice shelf hits the bedrock has been gradually increasing with time, indicating that the ice shelf beneath the station has been gradually thickening. This development is likely the main explanation why temporal minima in Figure 3 have become higher with time. At the same time the ice shelf next to Grímsfjall has thinned, most intensively near the recent eruption sites where at present the lake is partly free of glacier ice as evident in Figure 2. For this reason, the lake is presently deepest next to these eruption sites but not below the station on the ice shelf. Consequently, since 2004, the ice shelf beneath the station subsides all the way to the underlying bedrock before the lake is fully drained. It has been observed from elevation mapping of Grímsvötn (unpublished data of IES, deduced from Pléiades satellite images), that at present the station starts rising when ∼0.05 km^3 has accumulated in the lake, and the lake area is ∼4 km^2. This explains the periods of stable low elevation in Figure 3; the lake volume is then not sufficient to lift the sta-

tion. It is also known from the same data that when the lake drains completely the lake level has dropped below 1320 m a.s.l. resulting in ∼70 m greater pressure drop than indicated by the station. This happened e.g., during the jökulhlaup in 2021. The area undergoing pressure relief of such magnitude is, however, relatively small (∼1 km^2).

Taking the above into consideration, the values of lake level drop during jökulhlaups (Table 1) should be considered as minimum values, it is generally not known how far the lake level dropped below the lake level sensed by the station, during the listed jökulhlaups. This development also adds some degree of uncertainty to estimates of the drained water volume during the jökulhlaups. Generally, this is more likely to result in a slight underestimate, up to ∼0.05 km^3.

Spectral analysis

Samples of the tremor were isolated from suitable raw seismograms and analyzed with respect to frequency. Spectral analysis was done with the *Python* programming language's *ObsPy* and *NumPy* packages. Two-minute samples of the vertical seismogram from two of the stations operated by the Icelandic Meteorological Office, GRF on the caldera rim and KAL at a distance of 55 km (Figure 1), were selected in such a way that no earthquakes or other disturbances were visually present. Once appropriate snippets had been isolated they were each normalized to facilitate visual comparison of the frequency distribution. Then a highpass filter was applied at 0.7 Hz (highpass() method from the *ObsPy* package). This was done to minimise the effects of the oceanic microseisms (Gudmundsson *et al.*, 2007). All the unfiltered spectra show a prominent and persistent peak at low frequency, 0.15–0.2 Hz. This peak is also seen at most stations in Iceland irrespective of distance to volcanoes and is the familiar microseisms peak caused by the swell on the North Atlantic Ocean. Next numpy.fft.rfft() was used to calculate the Fast Fourier Transform. Finally smoothing was applied by convolving the absolute values of the spectrum with a constant vector of length 10, thereby calculating a moving average. This was done with *NumPy's* convolve() method.
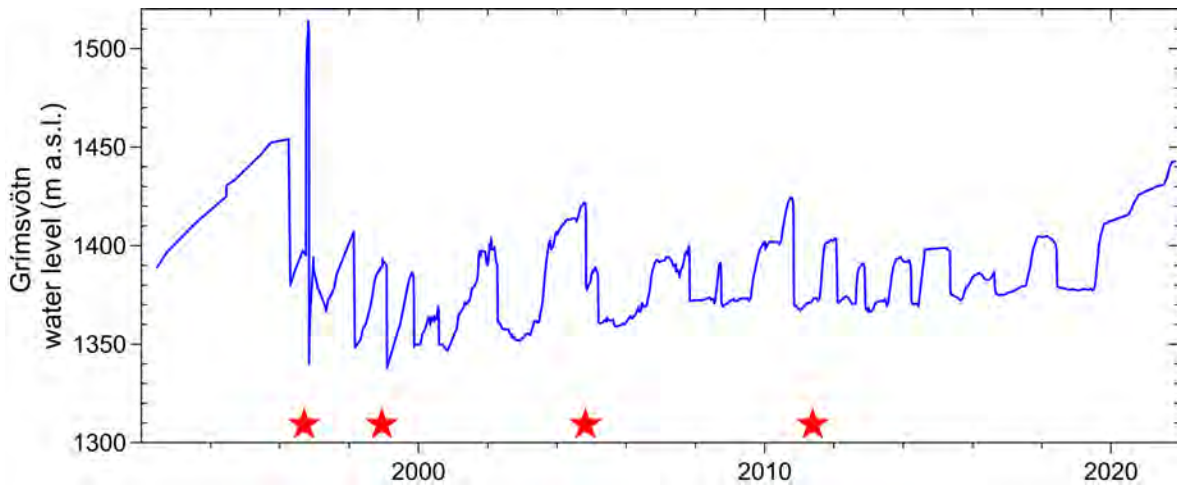
Figure 3. Water level in the Grímsvötn caldera lake 1992–2021 as inferred from the elevation of the ice shelf. The eruptions of Gjálp 1996, and Grímsvötn 1998, 2004 and 2011 are marked with red stars. Jökulhlaups are generally associated with rapid subsidence of the water level and ice shelf of the caldera lake. – *Vatnshæð í öskjuvatni Grímsvatna á tímabilinu 1992–2022 fundin út frá hæð íshellunnar. Rauðar stjörnur merkja tíma gosanna í Gjálp 1996, og Grímsvötnum 1998, 2004 og 2011. Jökulhlaup verða þegar vatnsborð og hæð íshellunnar á öskjuvatni Grímsvatna fellur ört.*

Table 1. List of jökulhlaups and eruptions from Grímsvötn caldera 1983–2021, with initial water level height, total drop of water level, and estimated water volume of the jökulhlaup (Björnsson, 2017; Pálsson and Magnússon, 2022). – *Listi yfir jökulhlaup og eldgos í Grímsvatnaöskjunni 1983–2021. Vatnshæð fyrir hlaup, heildarsig og rúmmál hlaupvatnsins.*

year	month		water level	drop	volume	year	month		water level	drop	volume
			m a.s.l.	m	km^3				m a.s.l.	m	km^3
1983	5	eruption				2004	10	jökulhlaup-eruption	1422	≥44	≥0.6
1983	12	jökulhlaup	1412	42	0.6	2005	3	jökulhlaup	1385	25	0.2
1984	8	(eruption)				2007	10	jökulhlaup	1400	28	0.3
1986	8	jökulhlaup	1430	80	1.2	2008	9	jökulhlaup	1391	22	0.2
1991	11	jökulhlaup	1452	82	1.5	2010	10	jökulhlaup	1419	49	0.6
1996	4	jökulhlaup	1454	75	1.2	2011	5	eruption			
1996	11	jökulhlaup after Gjálp	1510	175	3.2	2012	1	jökulhlaup	1405	35	0.4
1998	2	jökulhlaup	1407	59	0.5	2012	11	jökulhlaup	1388	21	0.2
1998	12	eruption				2014	3	jökulhlaup	1392	22	0.2
1999	1	jökulhlaup	1390	52	0.3	2015	5	jökulhlaup	1398	24	0.2
1999	9	jökulhlaup	1386	37	0.2	2016	8	jökulhlaup	1386	10	0.1
2000	7	jökulhlaup	1369	19	0.1	2018	6	jökulhlaup	1400	21	0.2
2001	12	jökulhlaup	1397	7	0.1	2021	11	jökulhlaup	1443	∼90	1.0
2002	2	jökulhlaup	1399	38	0.3						

Course of events

The course of events at Grímsvötn 1992–2021 is summarized by plotting the water level in the Grímsvötn caldera lake against time (Figure 3 and Table 1). The eruptions of 1998, 2004 and 2011, as well as the Gjálp eruption in 1996, are marked on the timeline in the figure. The choice of parameters in Figure 3 and Table 1 is governed by the types of processes that appear to be characteristic for the activity of this subglacial volcano, i.e. eruptions, inflation and deflation

of the volcano, and jökulhlaups from the caldera lake. Seismicity increases during periods of inflation, and then abruptly decreases as an eruption and deflation set in (Sturkell *et al.*, 2003, 2006; Vogfjörð *et al.* 2005). Similar behaviour is seen in the water level of the caldera lake. The lake level rises continuously due to inflow of surface meltwater in summer from the $\sim$175 km^2 Grímsvötn water catchment and due to geothermal melting. The rise stops when a leak begins and the ice dam fails. The level falls rapidly when the water finds its way subglacially and is released in a flood, jökulhlaup, at the glacier margin onto the alluvial plain near the coast (Figure 1) (Björnsson 1992, 2010). Sometimes the glacier dam is damaged by the jökulhlaups and geothermal meltwater is not contained in the caldera for some time. Such periods are represented, for example, by irregularities in the water level curve following the 1996 Gjálp eruption north of the Grímsvötn caldera (Figure 3). The lake level rose rapidly because of meltwater flowing into the caldera from the powerful Gjálp eruption. The water was subsequently released in a very large jökulhlaup (3.6 km^3) three weeks later (Björnsson, 1997; Einarsson *et al.*, 1997; Guðmundsson *et al.*, 1997; 2004). The glacier dam has not completely healed after that event. In 2004, an eruption followed a jökulhlaup, evidently triggered by the pressure drop in the caldera. Such events are known from earlier, notably the 1922 and 1934 eruptions of Grímsvötn (Þórarinsson, 1974).

Seismic observations showed many common characteristics shared by the events of Table 1. The difficult logistics and harsh weather conditions, however mean that the quality of the observations is quite variable. We selected the following events for analysis of the tremor because of the completeness of the data, and consider them representative of the whole data set.

Jökulhlaup triggered an eruption in November 2004. High-frequency seismic tremor indicating a beginning water flow from Grímsvötn was first detected on October 27, as seen in the blue curve in Figure 4. The amplitude gradually increased and on October 29 the flood had reached the glacier edge. An intense earthquake swarm was detected on November 1 and was immediately identified as a likely precursor to an eruption (Einarsson, 2018). The earthquake activity subsided towards the evening and was replaced by continuous, low-frequency, volcanic tremor, shown by the red curve in Figure 4, interpreted to mark the beginning of the eruption. The basaltic eruption broke out on a short fissure below the SW caldera rim when the water level had lowered by 10–15 m. Triggering of the eruption by the pressure release is considered very likely (Vogfjörð *et al.*, 2005). The amplitude of the volcanic tremor culminated in the early hours of November 2 and then gradually diminished, reaching background values on November 5, which presumably marks the end of the eruption. The jökulhlaup continued through and after the eruption and by the time it ended the ice shelf had subsided 44 m, corresponding to 0.55 km^3 of water drained from the caldera lake. The total volume of the eruptive products (DRE) is estimated at 0.05 km^3 (Oddsson *et al.* 2012).

Small jökulhlaup in 2008. The height of the ice shelf remained almost constant for months. Either very little water could collect in the lake, keeping the lake at 1372 m a.s.l. as shown in Figure 3, or water was collecting elsewhere, as explained above. The situation eventually went back to normal and the level of the lake rose sharply during the later summer months. Gradually increasing high-frequency tremor on the Grímsfjall seismograph indicated a beginning flood out of Grímsvötn caldera on September 24, 2008. The flood followed similar course as in earlier events, reached the glacier edge a few days later, peaked and then followed a declining trend until it ended on October 1. The total subsidence of the ice shelf was $\sim$22 m, corresponding to a water volume of $\sim$0.19 km^3.

Jökulhlaup in 2010. The ice elevation again showed little change for several months following the 2008 jökulhlaup. The ice shelf level in Grímsvötn caldera began rising again in August 2009 and by the autumn of 2010 it had reached a level higher than prior to the last few jökulhlaups (Figure 3). At the same time it was clear that the inflation of the volcano was approaching a critical stage where a volcanic eruption might be triggered by a sudden drop in water level, similar to the scenario of 2004. The beginning of the
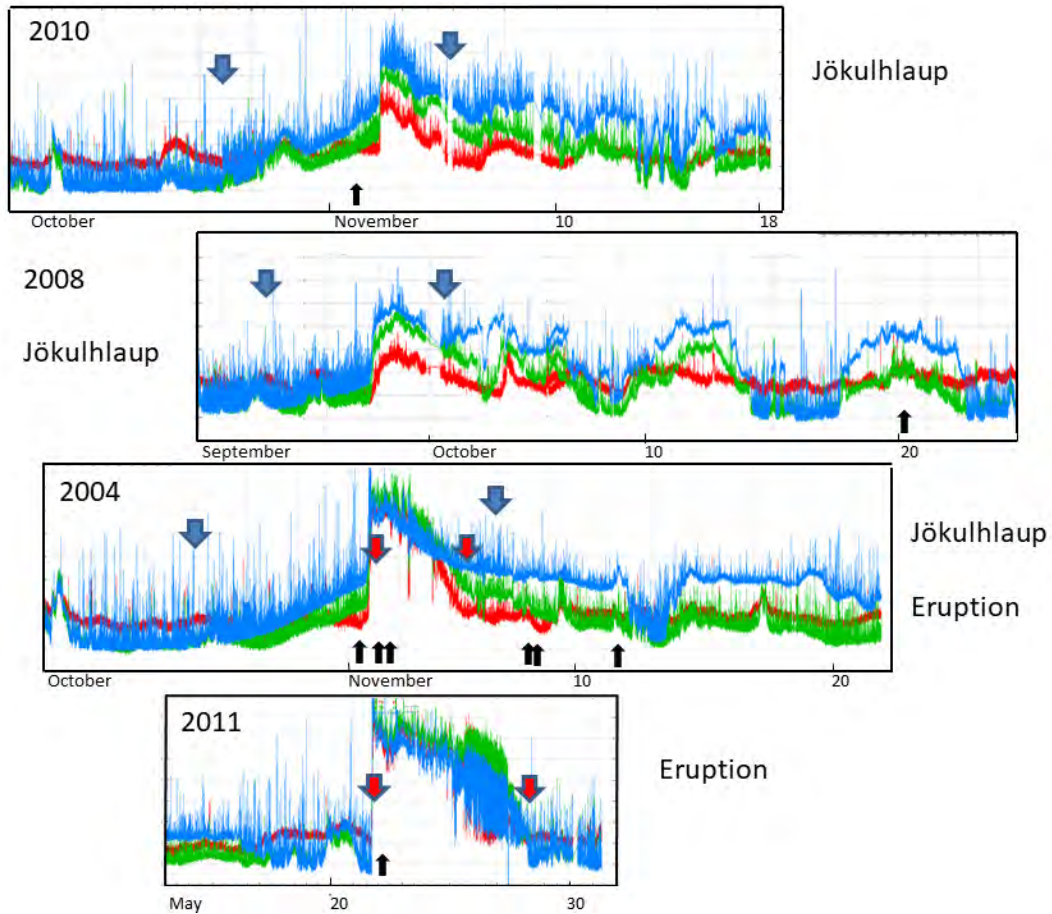
Figure 4. Tremorplots from the seismic station at Grímsvötn, GRF, for the four events of this study, the jökulhlaups of 2008 and 2010, and the eruptions of 2004 and 2011. The blue curve shows the spectral level for the 2–4 Hz frequency band, the green curve the spectral band 1–2 Hz, and the red curve the band 0.5–1 Hz. Blue arrows mark the beginning and end of the respective jökulhlaups, red arrows the beginning and end of the eruptions. Black arrows mark the time of the samples for the spectra in Figure 5. The vertical scale is arbitrary, but the same on all plots. – *Óróagröf frá skjálftamælinum á Grímsfjalli (GRF) fyrir atburðina fjóra sem fjallað er um í greininni, þ.e. jökulhlaupin 2008 og 2010, og eldgosin 2004 og 2011. Bláa línan sýnir styrk óróans á tíðnibilinu 2–4 Hz, græna línan styrkinn á tíðnibilinu 1–2 Hz, og rauða línan styrkinn á tíðnibilinu 0,5–1 Hz. Bláar örvar marka byrjun og endi jökulhlaupa, rauðar örvar byrjun og endi eldgosa. Svartar örvar marka tímann á sýnum fyrir tíðnirófin á mynd 5. Lóðrétti ásinn sýnir ótilgreindar einingar en er hinn sami á öllum gröfunum.*

water flow out of the caldera was seen on elevation changes of the ice shelf on October 23 and then later, on October 27 by a gradual rise in the amplitude of high-frequency tremor recorded at the Grímsfjall seismograph. The flood was verified at the glacier edge by October 29 (Einarsson *et al.*, 2016). The flood peaked on November 3 and then waned rather quickly, as is usual in normal jökulhlaups from Grímsvötn and was mostly over on November 5. No eruption broke out. The total subsidence of the ice shelf was ∼49 m corresponding to ∼0.55 km^3 of water released from the caldera lake.
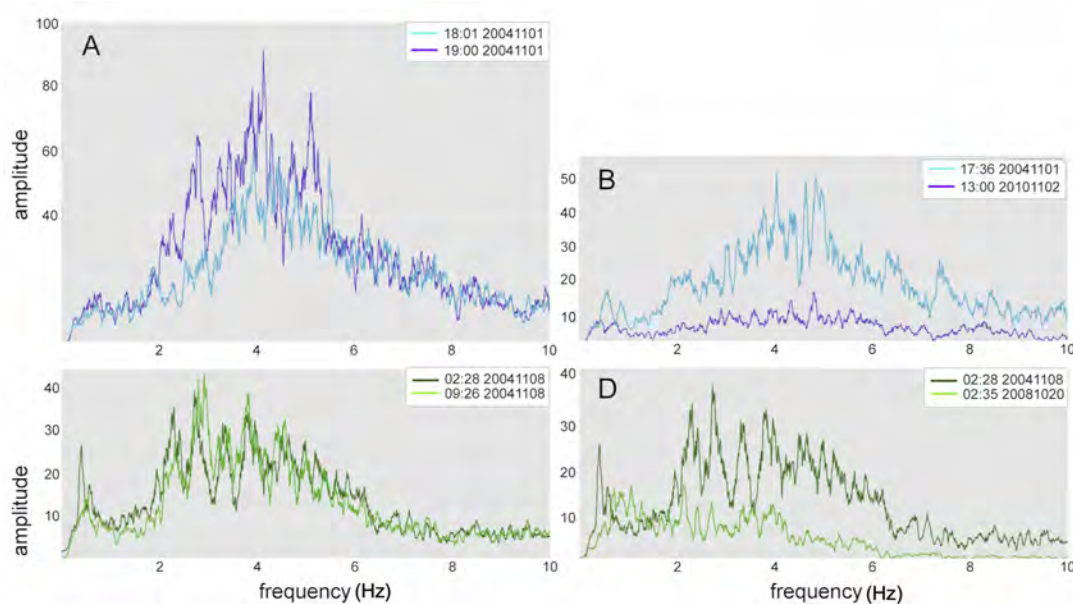
Figure 5. Spectral amplitude of specific types of tremor. Horizontal axis shows frequency in Hz, the vertical axis relative spectral level of the vertical velocity seismogram. A. Flood tremor at GRF during the jökulhlaup preceding the 2004 eruption, at 18:01 h (light blue) and 19:00 h (violet) on November 1. B. Flood tremor of two jökulhlaups compared, 2004 (light blue) and 2010 (violet). C. Geothermal tremor at GRF following the eruption of 2004, at 09:26 h (light green) and 02:28 h (dark green), both on November 8. D. Geothermal tremor of two jökulhlaups compared, 2004 (dark green) and 2008 (light green). – *Tíðniróf skjálftaóróa af mismunandi uppruna. A. Vatnsórói á skjálftastöðinni GRF meðan á jökulhlaupi stóð, á undan eldgosinu 2004, klukkan 18:01 (ljósblá lína) og 19:00 (fjólublá lína) 1. nóvember. B. Vatnsórói frá tveimur jökulhlaupum borinn saman, 2004 (ljósblár) og 2010 (fjólublár). C. Jarðhitaórói á mælinum á Grímsfjalli GRF eftir gosið 2004, klukkan 09:26 (ljósgrænn) og 02:28 (dökkgrænn), 8. nóvember. D. Jarðhitaórói eftir jökulhlaupin 2004 (dökkgrænn) og 2008 (ljósgrænn).*

Eruption in 2011. The inflation level of the volcano remained high following the jökulhlaup of 2010 and continued rising. The earthquake activity also increased. The magma chamber walls were finally breached on May 21 as marked by an intense earthquake swarm in the caldera and onset of deflation (Einarsson, 2018). The swarm started about 17:30 h. Continuous, low-frequency tremor increased shortly thereafter and culminated at 19 h. An eruption plume was seen at about 19 h (Hreinsdóttir *et al.*, 2014). The eruption culminated in the evening of May 21 and early hours of May 22, during which the eruption plume several times exceeded 20 km height. The eruption vigor quickly diminished, however, and by May 28, at 7 h, the eruption ended as judged from the tremor at Grímsfjall station. The eruption occurred in the SW corner of the caldera, a little west of the eruption site of 2004 (Figure 2). Earthquake activity in the caldera was low following the initial swarm. A few earthquakes were located in the caldera and to the W and NW of it, towards the subglacial Loki Ridge, the location of the E- and W-Skaftá Cauldrons (E and V in Figure 1).

Tremor characteristics

By comparing the tremorgraphs obtained during these jökulhlaups and eruptions with the course of events (Figure 4) three types of tremor can be identified:

Type 1: Tremor is clearly identified in all three jökulhlaups, 2004, 2008, and 2010, beginning about the time or shortly after the ice shelf begins to subside. This type of tremor is best seen on the blue
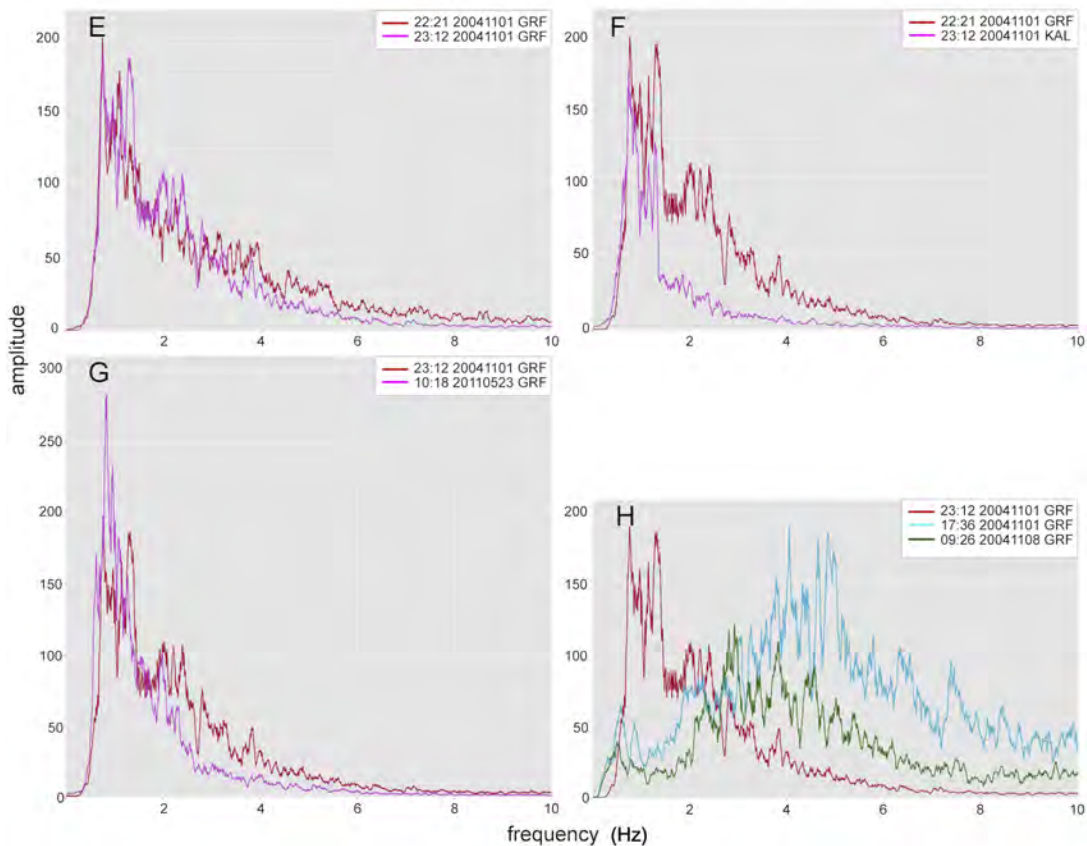
Figure 5 cont. E. Eruption tremor during the 2004 eruption, at 22:21 h (red) and 23:12 h (purple), both on November 1. F. Spectrum of eruption tremor of 2004 at two stations, GRF (red) and KAL (purple). G. Eruption tremor of two eruptions compared, 2004 (red) and 2011 (purple). H. Spectra of the three types plotted together, flood tremor (blue), geothermal tremor (green), and eruption tremor (red). *E. Gosórói meðan á eldgosinu 2004 stóð, klukkan 22:21 (rauður) og 23:12 (fjólurauður), 1. nóvember. F. Gosórói 2004 á tveimur mælistöðvum, GRF (rauður) og KAL (fjólurauður). G. Gosórói frá tveimur gosum borinn saman, 2004 (rauður) og 2011 (fjólurauður). H. Órói af þremur mismunandi gerðum borinn saman, vatnsórói (blár), jarðhitaórói (grænn) og gosórói (rauður).*

line in Figure 4. The signal consists of two components, i.e. a slowly varying background and superimposed spikes or cracking events. On the compressed time scale of the tremorgraphs this looks like a field with a solid bottom defined by the background noise and a fuzzy top made by the spikes. The tremor is thus represented by the lower edge of the blue field. The amplitude increases smoothly with increasing subsidence rate of the shelf. It is first seen on the high-frequency (blue) plot and then also on the intermediate-frequency graph (green). The low-frequency curve (red) appears to be unaffected. The spikes on the blue curve are due to small seismic events in the central region of the volcano and also ice cracking in the ice shelf and glacier surrounding the volcano. Note the high spike activity before the 2004 and 2010 jökulhlaups, compared to the 2008 jökulhlaup. This most likely reflects the microearthquake activity, and thus the level of inflation of the volcano prior to these jökulhlaups. The smoothly increasing tremor signal prior to the eruption in 2004 is assumed to be entirely due to water flow past the seis-

mograph at GRF through the caldera opening. Similar signals have been recorded during the initial phase of all jökulhlaups from Grímsvötn, the events of our study, in particular. We suggest the term flood tremor for this type.

Type 2: The tremor changes its characteristics suddenly when the lake level has dropped a certain amount. In the 2010 case this critical drop was 30 m, in 2008 it was 11 m and in 2004 it was 10–15 m. In an additional jökulhlaup in 2012 this critical drop was 18 m (Pálsson and Björnsson, 2013). The amplitude increases rather suddenly, even on the lowest frequency band, which has been little affected until then. The level of this tremor remains high for a day or so and then declines gradually, but it remains after the jökulhlaup has ended. It therefore does not seem to be caused by the water flow past the seismometer. Its amplitude may change suddenly, almost like it is turned off and on. This switching, as seen in Figure 4, is particularly clear in the 2008 case, and may continue for weeks after the jökulhlaup. Following the 2004 jökulhlaup and eruption, the switching off is seen on November 12, when the tremor level suddenly went temporarily back to the background microseismic level. The relative level of the three bands is always the same during this type of tremor: The high-frequency band is on top, then the intermediate-band, and the low-frequency band on the bottom. The less spiky appearance of this tremor during and after the jökulhlaup of 2008 compared to those of 2004 and 2010 may reflect less icequake activity associated with the smaller jökulhlaup or lower microearthquake background due to lower level of inflation of the volcano in 2008. The physical source of this tremor type is not obvious. It sets in about the time when most of the water has drained from the caldera, and there are no indications of eruptive activity. It does not seem to be related to the aftermath of eruptive activity either, because it did not appear after the large eruption of 2011. We suggest that it may be an expression of flash boiling in the geothermal system of Grímsvötn volcano, and coin the term geothermal tremor for it. The sudden beginning and end of the tremor episodes is consistent with the sudden phase changes when boiling sets in and stops.

Type 3: The tremor during the eruptions of 2004 and 2011 is quite distinct. All three frequency bands respond immediately when the eruption begins, and the amplitude level is about equal. It remains at the same level in all bands during the first phase of the eruption, then declines slowly. But as soon as the eruption is over the level changes, to the level of geothermal tremor in case of the 2004 eruption, and to the background level in case of the 2011 eruption. We identify this tremor type as eruption tremor.

Spectra of the tremor types

Samples of the three types of tremor were isolated and analyzed with respect to frequency. The results are presented as amplitude spectra in Figure 5. Additional normalization of the results was applied for subfigure G to make the difference in frequency content more apparent.

Type 1 (Flood tremor): A broad spectrum at high frequency, between 1.5–9 Hz is a characteristic of the flood tremor (Figure 5A). The two spectra, taken during the 2004 jökulhlaup at two different times during the period of increasing amplitude, have similar shape. The amplitude increases for increasing frequency, reaches a peak at 3.9–4.2 Hz and then decreases. The curve is roughly symmetrical about the peak. The main difference between the two spectra is subsidiary peaks on the stronger (and later) spectrum on either side of the peak, at 2.8 Hz and 5.2 Hz. These peaks do not appear to persist. The shape of the spectra of the flood tremor is similar for different jökulhlaups, as shown in Figure 5B.

Type 2 (Geothermal tremor): The tremor of type 2 (Figure 5C and 5D) has a frequency band between 2 and 6 Hz and is strongly peaked, with prominent peaks at 2.2, 2.8, 3.4, and 3.8 Hz. Spectral peaks at higher frequencies may be present. These peaks persist with a remarkable repeatability.

Type 3 (Eruption tremor): The eruption tremor (Figures 5E and 5F) contains lower frequencies than both flood and geothermal tremor. This type of tremor is characterized by prominent spectral peaks in the 0.3–3 Hz frequency band. The spectral amplitude increases towards the lower frequency end of the spectrum, and significant amplitude extends down to at least 0.8 Hz. The lower margin of the spectrum is

difficult to determine as the lower end of the spectrum merges with the oceanic microseisms. Comparison of the eruption tremor at two stations in Figure 5F reveals the effects of attenuation on the spectra at increasing distances. The amplitude of the higher frequencies is attenuated faster than the amplitude at the lower end of the spectrum, an effect that is further demonstrated in Figure 6. The peaks in the spectrum of the eruption tremor are persistent (Figure 7), with constant frequencies, giving the spectrograms striped appearance.

The spectral differences of the three tremor types are brought forth in Figure 5H. The flood and geothermal tremor both have a wide spectrum, peaking at different frequencies, the flood tremor at about 4 Hz, the geothermal tremor at about 3 Hz. The eruption tremor is distinctly different. It has a strong low-frequency component in the spectrum, with increasing amplitude towards the low-frequency end.

Distance effects

The three types of tremor have different amplitude decay with respect to distance. This is to be expected because of their different frequency content. High frequencies decay faster than low frequencies in the Earth (e.g., Gutenberg, 1958). The low-frequency eruption tremor is therefore expected to be detectable to larger distances than the high-frequent water tremor. To test this we plot side-by-side the tremorgraphs of the 2004 eruption at three different stations (Figure 6). The stations SKR and KAL are at the distance from Grímsvötn of 50 and 55 km, respectively. On the GRF tremorgraph, which is the same as shown in Figure 4, the water tremor shown by the blue line begins to rise above the background noise and be visible on October 26. The green curve of the intermediate frequencies rises above the noise slightly later, on October 28. Both curves show a steady rise until the time of the earthquake swarm on November 1 that preceded the begin of the eruption (Vogfjörð *et al.*, 2005; Einarsson, 2018). Similar increase of tremor above the regular background cannot be seen on the tremorgraphs from SKR and KAL. On these stations the relative level of the different frequency bands remains the same during the days of the flood, except possibly for a few hours immediately before the onset

of the earthquake swarm. The relative level also returns to the same background values on these stations after the eruption. The tremor on GRF, on the other hand, shows a different behaviour. The blue curve (high frequency) remains at a high level for more than three weeks after both eruption and flood ended. It eventually did return to normal background.

Two conclusions can be drawn from this comparison. Of the three types of tremor only the eruption tremor reaches the distant stations, SKR and KAL. The water tremor and the geothermal tremor have both decayed below the detection level of these stations. Furthermore, the effect of increasing attenuation with frequency is evident in the remaining amplitude of the eruption tremor (Figure 6).

The variable decay of the tremor types may also have something to do with other effects, such as the depth of their generation and the partitioning of the tremor into surface waves and body waves. Tremor generated at depth is likely to decay slower than tremor generated at the surface, even if the frequency content is the same. This depends on the attenuation properties of the surface layers of the crust. Furthermore, body waves decay faster with distance than surface waves due to their geometrical spreading. A study of these effects is beyond the scope of this paper.

Spectrogram of the 2004 events

The 2004 jökulhlaup and the triggered eruption are the only events where all three types of tremor are verified. The three types of tremor can be separated by their characteristics, however, by plotting a spectrogram from the GRF seismogram. The precursory activity and the beginning of the eruption is clearly seen on November 1 (Figure 7a). The red band at the bottom of the spectrograms is an expression of the microseisms generated by the N-Atlantic swell and is unrelated to the volcano. Earthquakes are expressed by vertical bands. The water flow tremor is visible at the high-frequency end of the spectrum (1.5–9 Hz). The blue-to-green colors show the increasing amplitude of the tremor, until the intense earthquake swarm begins after 20 h. The earthquake activity decreases around 22 h and low-frequency tremor appears (0.3–3 Hz). Similar transition was also observed at the initiation of previous subglacial eruptions in
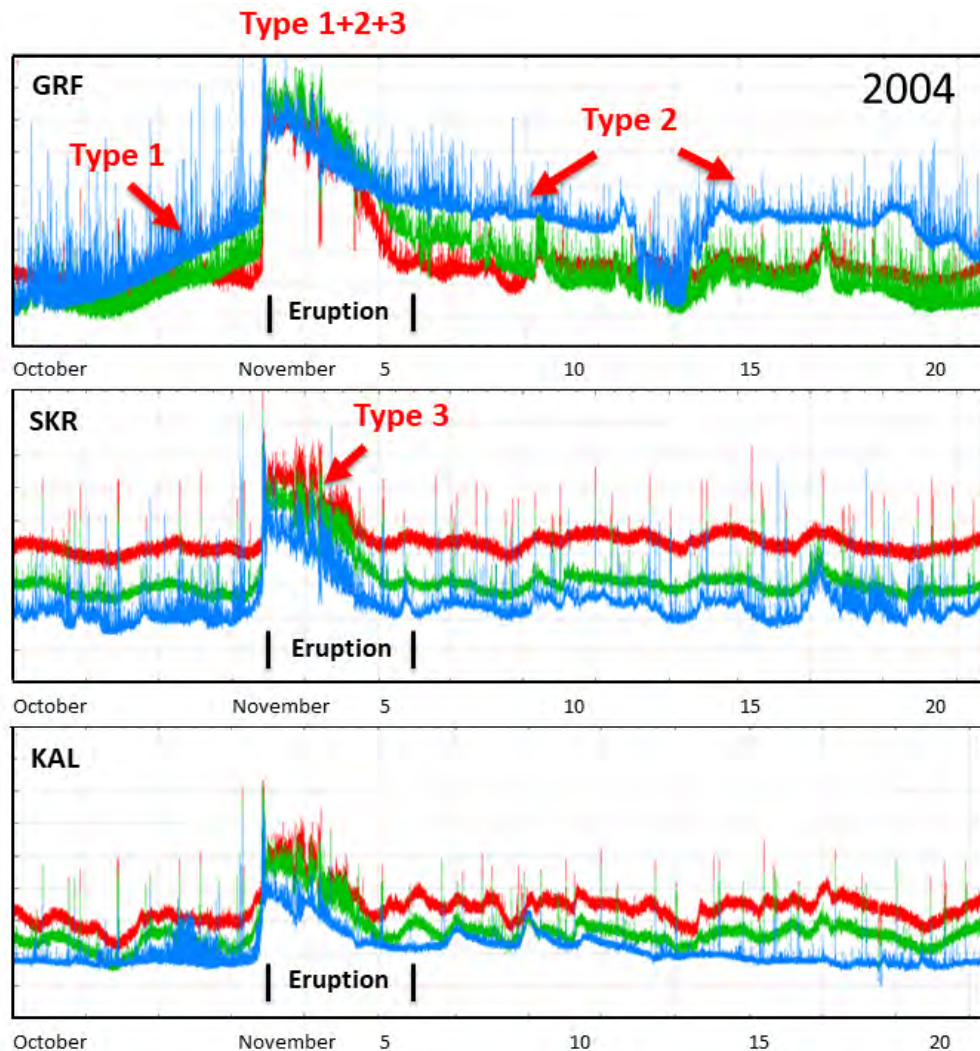
Figure 6. Tremor plots of the 2004 eruption recorded at three seismic stations at different distances from Grímsvötn. The color code for the different frequency bands is the same as in Figure 4. GRF is on the caldera rim of Grímsvötn, within a few kilometers of the eruption site, SKR is at the distance of 50 km WNW of the volcano, and KAL at 55 km to the SSW (Figure 1). The spikes with the red tops at SKR and KAL are low-frequency earthquakes originating on the west flank of the Katla volcano in S-Iceland at distances of 110 and 87 km, respectively. They belong to a sequence of events active for several decades (e.g. Soosalu *et al.*, 2006; Einarsson and Brandsdóttir, 2000; Sgattoni *et al.*, 2019), recently shown to be associated with a large, slow rock slide (Sæmundsson *et al.*, 2020). – *Óróagröf af eldgosinu 2004 og aðdraganda þess skráð á þremur skjálftamælistöðvum í mismunandi fjarlægð frá Grímsvötnum. GRF er á öskjubrún Grímsvatna, innan fárra kílómetra frá gosstöðvunum, SKR um 50 km VNV við eldstöðina, og KAL er 55 km SSV við Grímsvötn (mynd 1). Rauðu topparnir á óróagröfum SKR og KAL eru lágtíðniskjálftar sem áttu upptök við Tungnakvíslarjökul vestan Kötlu, í 110 og 87 km fjarlægð frá skjálftastöðvunum. Skjálftar hafa verið viðvarandi á þessum stað í marga áratugi og hefur nýlega komið í ljós að þeir tengjast fjallhrapi.*
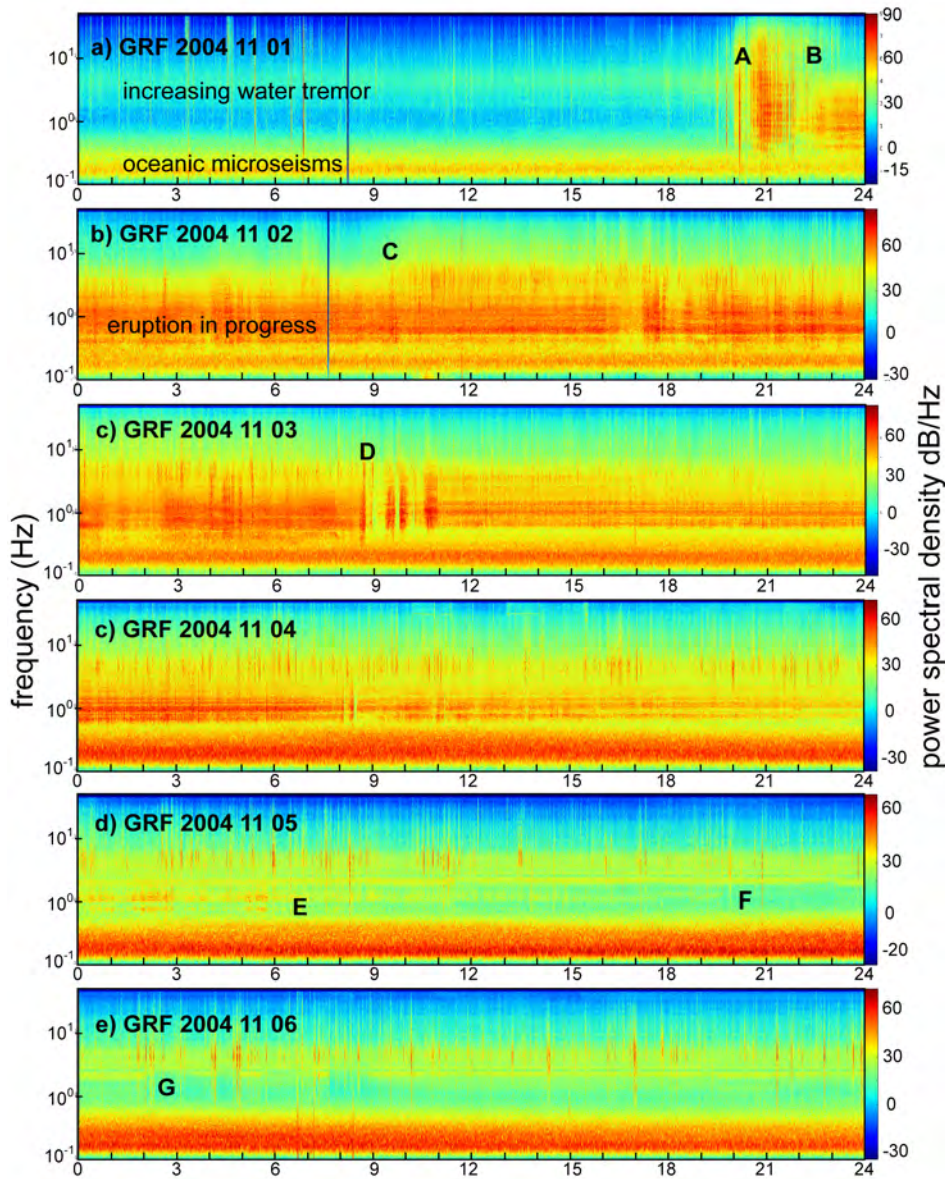
Figure 7. Spectrogram of the vertical component from the station GRF for November 1–6, 2004. A marks the beginning of the intense precursory earthquake activity, B the cessation of the earthquake activity and beginning of eruption tremor, C the widening of the tremor spectrum, and D disturbance and possible interruption of the eruption. E and F mark the end of the two peak spectral lines of the eruption tremor and G interruptions within the geothermal tremor. – *Tíðnirit af lóðrétta þætti skjálftamælistöðvarinnar á Grímsfjalli, GRF, fyrir dagana 1.–6. nóvember 2004. A sýnir byrjun skjálftahrinunnar í undanfara eldgossins. B merkir staðinn þar sem dregur úr skjálftum en stöðugur gosórói hefst. Við C víkkar tíðnisvið óróans og við D verður tímabundin truflun á gosóróanum, hugsanlega hlé á gosinu. E og F merkja lok tveggja meginþátta gosóróans. Við G sést truflun á jarðhitaóróanum.*

Grímsvötn 1983 (Einarsson and Brandsdóttir, 1984) and the Bárðarbunga-Gjálp eruption in 1996 (Einarsson *et al.*, 1997) and marks the end of the migration of magma at the beginning of the eruption (B in Figure 7a). The continuing eruption is expressed on the spectrogram of November 2 (Figure 7b). The spectral peaks and troughs shown in Figure 5 are invariant, giving the spectrogram striped appearance. The eruption tremor shows some variability in amplitude, and the spectrum widens at about 10 h (C in Figure 7b).

The striped appearance becomes even more pronounced on November 3 (Figure 7c) with decreasing amplitude, most likely reflecting decreasing intensity of the eruption. The frequencies of the bands appear to be constant, however. A pronounced disturbance in the activity is noticeable between 8 h and 11 h (D in Figure 7c), possibly temporary cessation of the eruptive activity. The tremor then resumes, but without the lowest band. The intensity of the eruption tremor continues decreasing on November 4 (Figure 7d). The eruption became very weak in the morning on November 5 and ended later that day. The two lowest spectral lines on the spectrogram in Figure 7d (0.7 Hz and 1.3 Hz) end at about 8 h and 19:40, which probably marks the end of the eruption (E or F in Figure 7d). These frequencies correspond to the two prominent peaks in the eruption tremor, seen in Figure 5D. The higher spectral lines of the tremor do not end, however, but fade out towards the end of next day (Figure 7f). They have frequencies of 2.1 Hz, 2.7 Hz, 3.3 Hz etc., and correspond to the peaks visible in the geothermal tremor in Figure 5C, shown in Figure 4. The lowest of these continuing spectral lines shows an interesting behavior on November 6 between 2 h and 9 h (G in Figure 7f). During that time interval it stops suddenly four times and begins again after 1/2 to one hour. This behavior is similar to that described earlier as characteristic for the geothermal tremor.

DISCUSSION

Three of the most active volcanoes in Iceland are covered to a large extent by glaciers, Katla, Bárðarbunga and Grímsvötn, several of the less active ones as well. The relatively frequent subglacial eruptions in Iceland are a source of a whole class of hazards different from other basaltic eruptions. Eruptions that would otherwise be relatively peaceful lava eruptions tend to be explosive and can lead to jökulhlaups, catastrophic floods of meltwater. These pose hazards to infrastructure such as roads, bridges, harbors, power lines, and pipelines for hot and cold water. Air traffic is severely influenced as well (e.g., Vogfjörð *et al.*, 2005; Barsotti *et al.* 2020). Effective and accurate monitoring of the activity of the volcanoes is therefore of vital importance. The seismic network is the primary tool for monitoring, on which most other monitoring methods rely. The inflation of a volcano that is going through preparatory stages for an eruption is likely to be detected and identified by increasing seismicity (Einarsson, 1991, 2018). Geodetic and geochemical methods can then be applied to that particular volcano. Eruptions and water floods generate continuous tremor that is detectable by the seismic network. Tremor has been used on numerous occasions in Iceland to follow remotely a course of events during eruptive activity. The beginning of the subglacial eruption in Gjálp 1996 was, for example, determined on the basis of low-frequency tremor (Einarsson *et al.*, 1997; Guðmundsson *et al.*, 1997), later verified by surveillance from the air. The beginning of the flood from the Grímsvötn caldera, when the meltwater of Gjálp was released three weeks later, was also determined from the high-frequency tremor detected by the analog seismograph at Grímsfjall, on the caldera rim. The flood emerged from the glacier edge about 10 hours later and swept away the bridges on the main highway.

Another example of the use of tremor for monitoring is provided by the events on the east flank of Katla volcano in July 2011, when a jökulhlaup from the Mýrdalsjökull glacier destroyed the bridge on the main highway. The flood came from ice cauldrons that collapsed in the glacier in response to basal melting. No signs of an eruption were seen at the surface of the glacier. Two kinds of seismic tremor accompanied this event (Sgattoni *et al.*, 2017; 2019). One was clearly related to the water flow, the origin of the other is still debated. Its spectral content and range resembles that of the eruption tremor of the present study.

Tremor recorded during the 2010 eruption of Eyjafjallajökull in S-Iceland was used for monitoring of that important eruption from the glacier-covered summit of the volcano (Benediktsdóttir *et al.*, 2022; Caudron *et al.*, 2022) that seriously disrupted air traffic in Europe. The tremor during the eruption was dominated by surface waves in the frequency range 0.5–2 Hz and was recorded in a wide area around the volcano, similar to the eruption tremor we find from Grímsvötn. Interestingly, it was observed that tremor was less efficiently generated during times of purely explosive activity than during times of mixed eruption mode, when both explosive and effusive activity occurred.

The Skaftá Cauldrons NW of Grímsvötn (Figure 1) provide yet another case of application of tremor for monitoring. The cauldrons in the ice are caused by basal melting of the glacier by geothermal activity. The meltwater collects at the base of the glacier and is released in substantial jökulhlaups every 1–2 years. The Grímsvötn jökulhlaup of 2008 is an interesting case for comparison with Skaftá jökulhlaups. A few days after the Grímsvötn event a jökulhlaup was also issued from the Eastern Skaftá Cauldron (Figure 1). The flood reached a maximum at the water level gauge 60 km downstream (at Sveinstindur) at 6 h on October 11. It is commonly observed that jökulhlaups from the E and W Skaftá Cauldrons are followed by bursts of low-frequency tremor. One of these bursts is seen on the Grímsfjall seismograph in the afternoon of October 12 (Figure 8), superimposed on the geothermal tremor following the Grímsvötn jökulhlaup. The geothermal tremor increases on October 10 and is high until at least October 13. The low-frequency peak from Skaftá Cauldron stands out, particularly on the low-frequency line (red), showing that the Skaftá Cauldron tremor has significantly lower frequency than the boiling tremor at Grímsvötn, and is more similar to the eruption tremor. The amplitude of the Skaftá tremor pulse is also much higher than that of the Grímsvötn geothermal tremor, especially considering the difference in distance.

The tremor observations from the Grímsvötn volcano are special for the reason that the three kinds of tremor can be separated in time and traced to separate sources. It is known whether and when an eruption occurred. For the many cases of jökulhlaups from the Skaftá Cauldrons (Vanderhoof, 2023; Eibl *et al.* 2020) and Katla 2011 (Sgattoni *et al.* 2017), for example, this is not known. No signs of eruptions were visible above the ice cover. It is not possible to exclude the possibility that the tremor pulses at the end of Skaftá jökulhlaups are caused by small, subglacial eruptions. If compared to the Grímsvötn tremor, they resemble the eruption tremor rather than water or geothermal tremor, both regarding the frequency and range of recording. The same argumentation was applied by Sgattoni *et al.* (2019) to conclude that a small subglacial eruption may have occurred at Katla in 2011. The source areas of the jökulhlaups at both Skaftá and Katla are covered by a thick glacier (400–500 m) and it would take a substantial eruption to break the surface of the glacier. For comparison, it took 31 hours for the powerful subglacial Gjálp eruption of 1996 to reach the surface, through the 550 m thick ice (Guðmundsson *et al.*, 2004). The tremor pulses at Skaftá Cauldrons had duration of the order of an hour or less and at Katla the tremor lasted 22 hours (Sgattoni *et al.*, 2017).

An interesting case for comparison with the Skaftá Cauldron jökulhlaups is provided by the jökulhlaup in 2013 from an ice-dammed lake within the caldera of Kverkfjöll volcano (Figure 1). The flood apparently triggered explosive activity in the geothermal area that generated tremor pulses recorded to distances exceeding 64 km (Montanaro *et al.* 2016).

CONCLUSIONS

By comparing different combinations of jökulhlaups and eruptions of the Grímsvötn caldera with seismic tremor observations during the period 1998–2011 a pattern emerges that is exemplified by four events, the jökulhlaups of 2004, 2008 and 2010, and the eruptions of 2004 and 2011. Three distinctly different types of tremor are identified by their different spectral characteristics and temporal relationships to the course of events in the caldera.

1. Jökulhlaups from the Grímsvötn caldera lake are accompanied by high-frequency tremor. The frequency band is mostly between 2 and 9 Hz and the
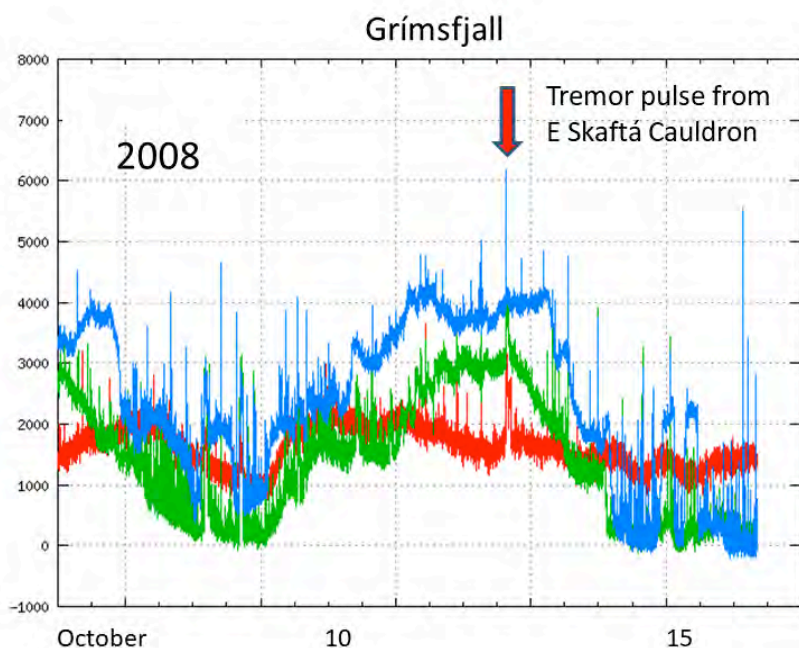
Figure 8. Tremorplot from the Grímsfjall seismograph October 6–16, 2008, showing the geothermal tremor from Grímsvötn following the jökulhlaup from Grímsvötn with the tremor pulse from the E Skaftá Cauldron on October 12 superimposed. *– Óróagraf frá skjálftastöðinni á Grímsfjalli 6.–16. október 2008 sem sýnir jarðhitaóróann frá Grímsvötnum í kjölfar jökulhlaupsins úr Grímsvötnum. Á grafinu sést einnig óróapúls frá Eystri Skaftárkatli sem varð 12. október í kjölfar hlaups úr katlinum.*

amplitude increases as the outflow rate increases. The amplitude decays rather rapidly with distance, and the tremor is rarely seen on seismic stations outside the glacier area.

2. When the water surface in the caldera lake falls below a certain (but slightly variable) level a second type of tremor sets in and is superimposed on the jökulhlaup tremor. The frequency band of this tremor is between 2 and 6 Hz and this tremor has a rather short range. It is rarely recorded outside the area of the glacier. It remains after all water flow and eruptive activity has ceased. Then it seems to be turned off and on rather abruptly several times. This tremor has several persistent spectral peaks. We postulate that this tremor is caused by flash-boiling in the geothermal system of the caldera.

3. Eruptions are accompanied by a third kind of tremor that sets in simultaneously with the eruptions. The frequency band of the eruption tremor is 0.5–4.0 Hz and it has a significantly longer range than the other types of tremor. It is recorded at stations out to a distance of at least 100 km. The eruption tremor has persistent spectral peaks, at least as recorded in the nearfield at the station GRF on the caldera rim.

ÁGRIP

Eiginleikar skjálftaóróa í tengslum við umbrot í megineldstöðinni í Grímsvötnum

Grímsvatnaeldstöðin er meðal virkustu eldstöðva landsins. Hún er að mestu leyti hulin jökli. Auk eldsumbrota er eldstöðin þekkt fyrir aflmikið jarðhitakerfi. Samspil jarðhita, eldvirkni og jökulsins býður upp á fjölbreytilega hegðun og náttúrufyrirbrigði sem óvíða er hægt að rannsaka. Jarðhitinn bræðir jökulinn og bræðsluvatnið auk yfirborðsbráðar af vatnasviði Grímsvatna safnast fyrir í öskju eldstöðvarinnar. Vatnshæðin vex þar til vatnið brýst undir jökulstífluna og úr verða jökulhlaup sem ryðja sér leið undir jöklin-

um og koma undan honum á Skeiðarársandi. Auk þess safnast kvika í kvikuhólf eldstöðvarinnar undir öskjunni með reglubundnum hætti og leiðir kvikusöfnunin til eldgosa þegar ákveðnum þrýstingi er náð. Stundum geta jökulhlaupin verkað eins og gikkur á eldvirknina. Ef kvikuþrýstingur er hár getur þrýstingslækkun í öskjuvatninu hleypt af stað eldgosi. Þetta gerðist í gosunum 1922, 1934 og 2004. Jökulhlaup áttu hins vegar ekki þátt í gosunum 1983, 1998 og 2011. Flest hlaup verða þó án þess að gos fylgi, t.d. 2008 og 2010. Allri þessari virkni fylgir svokallaður skjálftaórói, þ.e. stöðugur titringur sem kemur fram á skjálftamælum. Sérstaklega mælist óróinn vel á skjálftamæli á Grímsfjalli sem er staðsettur á öskjubarminum, rétt við útfall vatnsflóðanna úr öskjunni. Borin hafa verið kennsl á a.m.k. þrjár tegundir af óróa. Vegna þess hve fjölbreytileg virknin í Grímsvötnum er má tengja þessar tegundir við ákveðnar tegundir virkni:

1. Vatnsórói. Alltaf þegar koma jökulhlaup úr Grímsvötnum mælist hátíðniórói sem fer vaxandi í byrjun með reglubundnum hætti. Hann hefur stundum verið notaður sem fyrsta viðvörun um að hlaup sé að hefjast úr Vötnunum enda kemur hann fram á skjálftamælinum á Grímsfjalli talsvert áður en flóðsins verður vart á Skeiðarársandi. Vatnsóróinn er frekar skammdrægur og sést illa eða ekki á skjálftamælum utan Vatnajökuls.

2. Jarðhitaórói. Nánast alltaf þegar hlaup koma úr Grímsvötnum kemur fram önnur tegund óróa sem hvorki tengist vatnsrennsli né gosvirkni. Þetta er hátíðniórói með nokkuð stöðugu útslagi sem vex og minnkar skyndilega, næstum eins og slökkt sé og kveikt á honum á víxl. Óróinn byrjar nokkuð snögglega þegar vatnsborð Grímsvatna hefur sigið 10–30 m. Þetta ástand getur varað í allmarga daga eftir að hlaup og gos eru um garð gengin. Giskað hefur verið á að þessi órói tengist hvellsuðu í jarðhitakerfi Grímsvatna. Þessi tegund óróa, jarðhitaórói, er einnig frekar skammdræg og kemur lítið eða ekki fram á mælum utan Vatnajökuls.

3. Gosórói. Þegar eldgos hefst má sjá á skjálftamælum þriðju dæmigerða tegund óróa, gosóróa. Hann hefur frekar lága tíðni og má þannig aðgreina frá bæði vatnsóróanum og jarðhitaóróanum. Hann hefur ekki mælst nema þegar eldgos eru uppi, t.d. 2004 og 2011.

Gosórói berst lengra frá upptökum sínum en hinar tegundirnar tvær. Hann getur mælst langt út fyrir mörk Vatnajökuls. Þar ræður tíðni hans nokkru, en önnur áhrif gætu komið til, svo sem jarðlagaskipan og dýpi upptaka óróans.

Acknowledgements

REFERENCES

Barsotti, S., B. Oddsson, M. T. Gudmundsson, M. Pfeffer, M. Parks, B. G. Ófeigsson, F. Sigmundsson, V. Reynisson, K. Jónsdóttir, M. J. Roberts, E. P. Heiðarsson, E. B. Jónasdóttir, P. Einarsson, T. Jóhannsson, Á. G. Gylfason, K. Vogfjörð 2020. Operational response and hazards assessment during the 2014–2015 volcanic crisis at Bárðarbunga volcano and associated eruption at Holuhraun, Iceland. *J. Volcanol. Geothermal Res.* 390, 106753. https://doi.org/10.1016/j.jvolgeores.2019.106753

Benediktsdóttir, Á., Ó. Guðmundsson, K. L. Li and B. Brandsdóttir 2022. Volcanic tremor of the 2010 Eyjafjallajökull eruption. *Geophys. J. Int.* 228, 1015–1037. https://doi.org/10.1093/gji/ggab378

Björnsson, H. 1988. Hydrology of ice caps in volcanic regions. *Soc. Sci. Isl.* 45, 139 pp.

Björnsson, H. 1992. Jökulhlaups in Iceland: characteristics, prediction and simulation. *Ann. Glaciology* 16, 95–106.

Björnsson, H. 1997. *Grímsvatnahlaup fyrr og nú. Gos og hlaup 1996.* bls. 61–77. (Ritstj. Hreinn Haraldsson). Vegagerðin. Reykjavík.

Björnsson, H. 2010. Understanding jökulhlaups: from tale to theory. *J. Glaciology* 56, No. 200, 1002–1010. https://doi.org/10.3189/002214311796406086

Björnsson, H. 2017. The Glaciers of Iceland: A Historical, Cultural and Scientific Overview. *Atlantis Advances in Quaternary Science* 2, 613 pp. https://doi.org/10.2991/978-94-6239-207-6

Björnsson H. and P. Einarsson 1990. Volcanoes beneath Vatnajökull, Iceland: Evidence from radio-echo sounding, earthquakes and jökulhlaups. *Jökull* 40, 147–168.

Bödvarsson, R., S. Th. Rögnvaldsson, R. Slunga and E. Kjartansson 1999. The SIL data acquisition system at present and beyond year 2000. *Phys. Earth Planet Inter.* 113, 89–101.

Brandsdóttir, B. and P. Einarsson 1992. Volcanic tremor and low-frequency earthquakes in Iceland. In: Gasparini P., R. Scarpa and K. Aki (eds.). *Volcanic seismology.* Springer-Verlag, Berlin Heidelberg, 212–222.

Caudron, C., J. Soubestre, T. Lecocq, R. S. White, B. Brandsdóttir and L. Krischer 2022. Insights into the dynamics of the 2010 Eyjafjallajökull eruption using seismic interferometry and network covariance matrix analyses. *Earth Planet. Sci. Lett.* 585, 117502. https://doi.org/10.1016/j.epsl.2022.117502

Eibl, E. P. S., C. J. Bean, B. Einarsson, F. Pálsson and K. S. Vogfjörd 2020. Seismic ground vibrations give advanced early-warning of subglacial floods. *Nature Comm.* 11(1). https://doi.org/10.1038/s41467-020-15744-5

Einarsson, B., E. Magnússon, M. Roberts, F. Pálsson, Th. Thorsteinsson and T. Jóhannesson 2016. A spectrum of jökulhlaup dynamics revealed by GPS measurements of glacier surface motion. *Ann. Glaciology* 57(72), 47–61. https://doi.org/10.1017/aog.2016.8

Einarsson, P. 1991. Earthquakes and present-day tectonism in Iceland. *Tectonophysics* 189, 261–279. doi.org/10.1016/0040-1951(91)90501-I

Einarsson, P. 2018. Short-term seismic precursors to Icelandic eruptions 1973–2014. *Front Earth Sci.* 6, 45.https://doi.org/10.3389/feart.2018.00045

Einarsson, P. 2019. Historic accounts of pre-eruption seismicity of Katla, Hekla, Öræfajökull and other volcanoes in Iceland. *Jökull* 69, 35–52. https://doi.org/10.33799/jokull2019.69.035

Einarsson, P. and B. Brandsdóttir 1984. Seismic activity preceding and during the 1983 volcanic eruption in Grímsvötn, Iceland. *Jökull* 34, 13–23.

Einarsson, P. and B. Brandsdóttir 2000. Earthquakes in the Mýrdalsjökull area, Iceland, 1978–1985: Seasonal correlation and connection with volcanoes. *Jökull* 49, 59–73.

Einarsson, P. and S. Jakobsson 2020. The analog seismogram archive of Iceland, scanning and preservation for future research. *Jökull* 70, 57–71. https://doi.org/10.33799/jokull2020

Einarsson, P., B. Brandsdóttir, M. T. Guðmundsson, H. Björnsson, K. Grönvold and F. Sigmundsson 1997. Center of the Iceland Hotspot experiences volcanic unrest. *Eos Transactions* 78, Sept. 2, 369–375. https://doi.org/10.1029/97EO00237

Gudmundsson, M. T., and H. Björnsson 1991. Eruptions in Grímsvötn, Vatnajökull, Iceland, 1934–1991. *Jökull* 41, 21–45.

Gudmundsson, M. T., F. Sigmundsson and H. Björnsson 1997. Ice-volcano interaction of the 1996 Gjálp subglacial eruption, Vatnajökull, Iceland. *Nature* 517, 191–195.

Gudmundsson, M. T., F. Sigmundsson, H. Björnsson and Th. Högnadóttir 2004. The 1996 eruption at Gjálp, Vatnajökull ice cap, Iceland: efficiency of heat transfer, ice deformation and subglacial water pressure. *Bull. Volcanol.* 66, 46–65.

Gudmundsson, Ó., A. Khan, P. Voss 2007. Rayleigh-wave group-velocity of the Icelandic crust from correlation of ambient seismic noise. *Geophys. Res. Lett.* 34 (14). https://doi.org/10.1029/2007GL030215.

Gutenberg, B. 1958. Rheological problems of the Earth's interior. In: *Rheology: Theory and Applications* (ed. F. R. Eirich) 2, 401–422. Academic Press, New York.

Hreinsdóttir, S., F. Sigmundsson, M. Roberts, H. Björnsson, R. Grapenthin, Þ. Arason, Þ. Árnadóttir, J. Hólmjárn, H. Geirsson, R. A. Bennett, M. T. Gudmundsson, B. Oddsson, B. G. Ófeigsson, T. Villemin, T. Jónsson, E. Sturkell, Á. Höskuldsson, G. Larsen, Th. Thordarson and B. A. Óladóttir 2014. Volcanic plume height correlated with magma-pressure change at Grímsvötn Volcano, Iceland. *Nature Geoscience* 7, 214–218. https://doi.org/10.1038/ngeo2044

Montanaro, C., B. Scheu, M. T. Guðmundsson, K. Vogfjörð, H. I. Reynolds, T. Dürig, K. Strehlow, S. Rott, T. Reuschlé, D. B. Dingwell 2016. Multidisciplinary constraints of hydrothermal explosions based

on the 2013 Gengissig lake events, Kverkfjöll volcano, Iceland. *Earth Planet. Sci. Lett.* 434, 308–319. http://dx.doi.org/10.1016/j.epsl.2015.11.043

Oddsson, B., M. T. Gudmundsson, G. Larsen and S. Karlsdóttir 2012. Monitoring of the plume from the basaltic phreatomagmatic 2004 Grímsvötn eruption – application of weather radar and comparison with plume models. *Bull. Volcanol.* 74, 1395–1407.

Pálsson, F. and H. Björnsson 2013. *Report on funds spent 2012 on research cooperation on jökulhlaups from Grímsvötn.* Institute of Earth Sciences, University of Iceland, Report, 14 pp.

Pálsson, F. and E. Magnússon 2022. *Greinargerð vegna styrks af tilraunafé árið 2021: Samvinna um rannsóknir í Grímsvötnum.* Institute of Earth Sciences, University of Iceland, Report RH-03-22.

Porter, C., P. Morin, I. Howat, M.-J. Noh, B. Bates, K. Peterman *et al.* 2018. ArcticDEM. Harvard Dataverse, V1. Polar Geospatial Center, University of Minnesota. https://doi.org/10.7910/DVN/OHHUKH

Sæmundsson, Þ., J. M.-C. Belart, P. Einarsson, H. Geirsson, Á. R. Hjartardóttir, E. Magnússon, F. Pálsson and G. B. M. Pedersen 2020. Slope deformation above the Tungnakvíslarjökull outlet glacier in western part of the Mýrdalsjökull glacier – causes and consequences. Nordic Geological Winter Meeting, January 8–10, 2020, Oslo, Norway. Abstract Volume.

Sgattoni, G., Ó. Guðmundsson, P. Einarsson, F. Lucchi, K. L. Li, H. Sadeghisorkhan, R. Roberts and A. Tryggvason 2017. The 2011 unrest at Katla volcano: Location and interpretation of the tremor source. *J. Volcanol. Geothermal Res.* 338, 63–78. https://doi.org/10.1016/j.jvolgeores.2017.03.028.

Sgattoni, G., F. Lucchi, P. Einarsson, G. De Astis and C. A. Tranne 2019. The 2011 unrest at Katla volcano: seismicity and geological context. *Jökull* 69, 53–70. https://doi.org/10.33799/jokull2019.69.053

Sigmundsson, F. and M. T. Gudmundsson 2004. Grímsvötn eruption, November 1–6, 2004. *Jökull* 54, 139–142.

Sigmundsson, F., M. Parks, R. Pedersen, K. Jónsdóttir, B. G. Ófeigsson, R. Grapenthin, S. Dumont, P. Einarsson, V. Drouin, E. R. Heimisson, Á. R. Hjartardóttir, M. T. Guðmundsson, H. Geirsson, S. Hreinsdóttir, E.

Sturkell, A. Hooper, Þ. Högnadóttir, K. Vogfjörð, T. Barnie and M. Roberts 2018. Magma movements in volcano plumbing systems and their associated ground deformation and seismic pattern. In: *Volcanic and Igneous Plumbing Systems*, (Ed. S. Burchardt), Chapter 11, 285–322, Elsevier. https://doi.org/10.1016/B978-0-12-809749-6.00011-X.

Soosalu, H., K. Jónsdóttir and P. Einarsson 2006. Seismicity crisis at the Katla volcano, Iceland – signs of a cryptodome? *J. Volc. Geotherm. Res.* 153, 177–186. https://doi.org/10.1016/j.jvolgeores.2005.10.013

Stefánsson, R., R. Böðvarsson, R. Slunga, P. Einarsson, S. Jakobsdóttir, H. Bungum, S. Gregersen, J. Havskov, J. Hjelme and H. Korhonen 1993. Earthquake prediction research in the South Iceland seismic zone and the SIL project. *Bull. Seismol. Soc. Am.* 83, 696–716.

Sturkell, E., P. Einarsson, F. Sigmundsson, S. Hreinsdóttir and H. Geirsson 2003. Deformation of Grímsvötn volcano, Iceland: 1998 eruption and subsequent inflation. *Geophys. Res. Lett.* 30(4), 1182. https://doi.org/10.1029/2002GL016460.

Sturkell, E., P. Einarsson, F. Sigmundsson, H. Geirsson, R. Pedersen, E. Van Dalfsen, A. Linde, S. Sacks and R. Stefánsson 2006. Volcano geodesy and magma dynamics in Iceland. *J. Volc. Geothermal Res.* 150, 14–34. https://doi.org/10.1016/j.jvolgeores.2005.07.010.

Þórarinsson, S. 1974. *Vötnin stríð. Saga Skeiðarárhlaupa og Grímsvatnagosa.* (The Swift Flowing Waters, the History of Floods in Skeiðará and Eruptions in Grímsvötn, in Icelandic). Bókaútgáfa Menningarsjóðs, Reykjavík, 254 pp.

Vanderhoof, B. E. 2023. *Characterizing tremor signals of the 2015–2021 Skaftárkatlar jökulhlaups.* University of Iceland, Faculty of Earth Sciences, M.Sc. Thesis, 98 pp.

Vogfjörd, K. S., S. S. Jakobsdóttir, G. B. Gudmundsson, M. J. Roberts, K. Ágústsson, Th. Arason, H. Geirsson, S. Karlsdóttir, S. Hjaltadóttir, U. Ólafsdóttir, B. Thorbjarnardóttir, Th. Skaftadóttir, E. Sturkell, E. B. Jónasdóttir, G. Hafsteinsson, H. Sveinbjörnsson, R. Stefánsson and Th. V. Jónsson 2005. Forecasting and monitoring of a volcanic eruption in Iceland. *Eos Transactions* 86, 26, 245–248.